



NUMBER OF SUBCARRIER FILTER COEFFICIENTS IN GFDM SYSTEM: EFFECT ON PERFORMANCE

NÚMERO DE COEFICIENTES DEL FILTRO DE LAS SUBPORTADORAS EN EL SISTEMA GFDM: EFECTO EN EL DESEMPEÑO

Randy Verdecia Peña^{1,*}, Humberto Millán Vega²

Abstract

Generalized Frequency Division Multiplexing (GFDM) is a non-orthogonal multicarrier transmission scheme proposed for fifth (5G) and future generation wireless networks. Due to its attractive properties, it has been recently discussed as a candidate waveform for the future wireless communication systems. GFDM is introduced as a generalized form of the widely used Orthogonal Frequency Division Multiplexing (OFDM) modulation scheme and it uses only one cyclic prefix (CP) for a group of symbols. The main focus of this work is to present like impact on the system performance the coefficient quantity of the subcarrier filter. A simple method for the computation of the coefficients of the prototype filter is employed. Besides, it is presented a structure for the GFDM by taking advantage of the arrangement in the modulation matrix. We evaluated the Bit Error Rate (BER) using the receiver models presented in this work. The results showed that the BER is affected according to the coefficients quantity of the prototype filter. Based on the obtained results, the coefficients quantity has a relation with the number of time slots of the GFDM system.

Keywords: GFDM, number of coefficients, prototype filter, BER.

Resumen

El GFDM (*Generalized Frequency Division Multiplexing*) es un esquema de transmisión multiportadora no ortogonal propuesta para la quinta (5G) y futura generación de redes inalámbricas. Por sus atractivas propiedades, está siendo investigada como una forma de onda a ser considerada para los futuros sistemas de redes de comunicaciones. La GFDM es introducida como una generalización del ampliamente utilizado esquema de modulación OFDM (*Orthogonal Frequency Division Multiplexing*) y usa un único prefijo cíclico (*Cyclic Prefix, CP*) para un grupo de símbolos. El objetivo principal de este trabajo es presentar cómo impacta la cantidad de coeficientes del filtro de las subportadoras en el desempeño del sistema. Se emplea un método simple para el cálculo de los coeficientes del filtro prototipo. Además, se presenta una estructura para la GFDM aprovechando la estructura de modulación matricial. Se evaluó la tasa de error de bit (*Bit Error Rate, BER*) usando los modelos de receptores presentados en este trabajo. Los resultados muestran que el BER es afectado según la cantidad de coeficientes del filtro prototipo. Basado en los resultados obtenidos, la cantidad de coeficientes tiene relación con el número de intervalos de tiempo del sistema GFDM.

Palabras clave: GFDM, número de coeficientes, filtro prototipo, BER.

^{1,*}Signals, Systems and Radiocommunications Department, Escuela Técnica Superior de Ingenieros de Telecomunicaciones (ETSIT), Universidad Politécnica de Madrid, España. Corresponding author ✉: randy.verdecia@upm.es

<http://orcid.org/0000-0003-4798-2681>

²Physical Department (Retired), Universidad de Granma – Cuba. <http://orcid.org/0000-0001-9421-7494>

Received: 25-06-2019, accepted after review: 25-11-2019

Suggested citation: Verdecia Peña, R. and Millán Vega, H. (2020). «Number of subcarrier filter coefficients in GFDM system: effect on performance». INGENIUS. N.º 23, (january-june). pp. 53-61. DOI: <https://doi.org/10.17163/ings.n23.2020.05>.

1. Introduction

Wireless and Mobile communication have become essential tools for the life and modern society. The future wireless networks of telecommunication need higher throughput based on very high spectral and energy efficiencies, very low latency and very high data rate. That requires a more effective physical layer (PHY) [1–3]. The core of the physical layer of fourth generation (4G) is the Orthogonal Frequency Division Multiplexing (OFDM). These systems allow high data throughput. OFDM modulation is widely adopted due to its favorable features like a simple implementation built on the Fast Fourier Transform (FFT) and robustness against fading channels [2, 4]. However, the application scenario previewed for fifth generation (5G) networks have challenges where OFDM could have limitations. The low latency needed for Vehicle to Vehicle Communications and Tactile Internet applications require a data cutoff where OFDM packet with one cyclic prefix (CP) per symbol have a low spectral efficient [1, 4–6]. The requirement of OFDM to preserve the orthogonality between individual subcarriers is essential for the machine-to machine (M2M) communication. Due to the need of low power consumption which influence the negative form on the synchronization process, this procedure is not possible by OFDM modulation [4, 7]. Other disadvantage of the OFDM system is the high out-of-band (OOB) radiation resulting from rectangular pulse shaping [8]. OFDM can fulfill the requirements of 5G in a limited way, due to these shortcomings.

In recent years, several waveforms have been proposed to overcome the above limitations of OFDM, this is the case of FBMC, UFMC, GFDM in references [9–14] are suggested many waveforms. Filter Bank Multicarrier (FBMC) the subcarriers are pulse shaped individually to reduce the OOB emissions, this is caused because the subcarriers have narrow bandwidth and the length of the transmit filter impulse response is long. The applications that to need a number of transmit of large symbols are benefit with this modulation. But it is clear, this modulation scheme is not suitable for low latency scenarios, where high efficiency must be achieved with short burst transmissions [1, 5–7]. Universal Filtered Multicarrier (UFMC) a group of subcarriers is filtered to reduce the OOB emission. A principal characteristic of this modulation is the impulse response can be short obtaining high spectral efficiency in short transmissions [1].

The disadvantage of UFMC does not require a CP, then is more sensitive to small time misalignment than CP-OFDM and might not be suitable for applications that need loose time synchronization to save energy [1, 5, 6]. In this context, the Generalized Frequency Division Multiplexing (GFDM) is one alternative multicarrier scheme that is currently under

evaluation as a candidate of the PHY layer for the next generation of mobile communication systems. It is interesting that one of the main relevance of the GFDM is that its generalized form of OFDM preserves most of the valuable properties of OFDM while addressing its limitations. The GFDM can provide a very low OOB radiation. It is more bandwidth efficient than OFDM as it uses only CP for group of symbols in its block rather than a CP per symbol as for the case of OFDM [9, 15].

The GFDM modulation is foreseen for the modulation of independent blocks where each block consists of a number of subcarriers and symbols. The data symbols belonging to the subcarriers are filters with a prototype that is circularly shifted in time and frequency domains. The subcarrier filtering results in non-orthogonal subcarriers, then inter-symbol (ISI) and inter-carrier (ICI) might arise. Filter Impulse Response (FIR) can be employed for filtering the subcarriers and this choice has a negative impact on the Bit Error Rate (BER) performance and the OOB emissions as shown in [1]. In this work, we present BER curves to compare the influence that to have the selection of the total number of coefficient's filter and is shown to exist a relationship between the number of time slots and the coefficients of the filter in the GFDM systems. It is necessary to present this aspect because performance degrades when the total coefficient is not chosen correctly.

A GFDM symbol consists of a block structure of MN samples, where each N subcarrier carries M timeslots. In a GFDM block, the overhead is kept small by adding a single CP for an entire block that contains multiple subcarriers. Thus period that benefit can be used to improve the spectral efficiency of the system. The remaining sections are organized as follows. The systems model and properties of the GFDM transmitter are presented in Section 2. Section 3 presents different receiver structures. Section 4 shows the expression of the prototype filter as obtained from the subcarrier filter coefficients. Section 5 analyzes the BER performance of GFDM including the theoretical equations assuming Zero-Forcing (ZF), Matched Filter (MF) and Matched Filter–Parallel Interference Cancellation (MF-PIC) receivers. We used the coefficients obtained in Section 4. Finally, Section 6 presents some conclusions. The main objective of this work is to present a structure for the GFDM by taking advantage of the arrangement in the modulation matrix.

Notation: Bold lower case is used for column vectors and bold upper case for matrices. All vectors are in column form. The vector and matrix transpose and Hermitian are indicated by the superscripts 'T' and 'H', respectively. We use \mathbf{W}_{MN} to denote the discrete Fourier transform (DFT) matrix of size MN. We also assume that \mathbf{W}_{MN} is normalized, such that $\mathbf{W}_{MN} \mathbf{W}_{MN}^H = \mathbf{I}_{MN}$, where \mathbf{I}_{MN} denotes the identity

matrix of size MN . Hence, $\mathbf{W}_{MN}^H = \mathbf{W}_{MN}^{-1}$. The terms FFT and iFFT refer to the fast implementation of DFT and inverse DFT (iDFT), respectively.

2. Materials and Methods

2.1. System model and properties of GFDM

The Generalized Frequency Division Multiplexing is a multicarrier system. The data packet in GFDM is such that only one CP per block of transmitted symbols is required [10]. Figure 1 presents the structure of a GFDM data packet. In the system GFDM the data symbols over each subcarrier are filtered through a well-localized band-pass filter with the aim of limiting the Inter-Carrier Interference (ICI) [16]. The GFDM data packet is organized in M time-slots and N subcarriers.

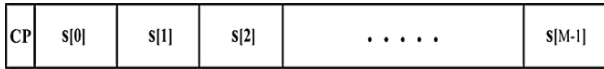


Figure 1. GFDM data packet.

The OFDM system can provide a high Out-Of-Band (OOB) radiation and a least bandwidth efficiency in comparison with GFDM [1, 8] due to the fact that OFDM system uses a CP per symbol as is presents in Figure 2.

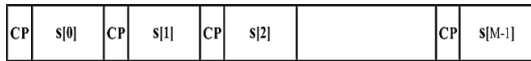


Figure 2. OFDM data packet.

Consider the block diagram of the transceiver depicted in Figure 3. A mapper, e.g QAM [7], maps the encoded bits to symbols from a 2^α valued complex constellation, where α is the modulation order. The \mathbf{s} vector denotes a data block that contains MN symbols, which can be decomposed into M time-slots and N subcarrier each according to $\mathbf{s} = [\mathbf{s}^T[0]\mathbf{s}^T[1], \dots, \mathbf{s}^T[M-1]]^T$ and $\mathbf{s}[m] = [s_0[m]s_1[m], \dots, s_{N-1}[m]]^T, m = 1, 2, \dots, M-1$.

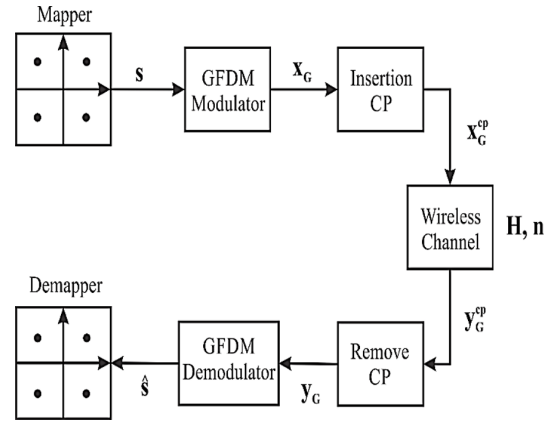


Figure 3. Block diagram of the transceiver for GFDM.

The data symbols are taken from a zero mean independent and identically distributed (i.i.d) process with unit variance. The expression that relates the input data symbols $\mathbf{s}[m]$ and GFDM transmitter output $\mathbf{x}[m]$, may be expressed as [16].

$$\mathbf{x}[m] = \mathbf{W}_{MN}^{-1} \mathbf{C}_f \mathbf{s}_{ex}[m], \quad m = 0, 1, 2, \dots, M-1 \quad (1)$$

where \mathbf{W}_{MN}^{-1} is the iDFT matrix of size $(MN \times MN)$, \mathbf{C}_f is circular matrix of the size $(MN \times MN)$, with the first column composed by the vector $\mathbf{c} = [c_0 \ c_1 \ \dots \ c_{F-1} \ 0 \ \dots \ 0 \ c_{F-1} \ \dots \ c_1]^T$. The coefficients c_f are the components of the discrete spectrum of the formatter pulse, with $f \in (0, 1, \dots, F-1)$ and $(1 \leq F \leq \frac{MN}{2})$ [17, 18]. It will be shown in this work that the coefficients quantity influences the GFDM system performance. $\mathbf{s}_{ex}[m]$ is the expanded vector of the data symbols $\mathbf{s}[m]$ that can be organized as $\mathbf{s}_{ex}[m] = [s_0[m]\mathbf{z}_{M-1}^T s_1[m]\mathbf{z}_{M-1}^T s_2[m]\mathbf{z}_{M-1}^T \dots \mathbf{z}_{M-1}^T s_{N-1}[m]]^T$, where \mathbf{z}_{M-1} represents the column vector of the size $(M-1 \times 1)$ [17, 18].

The expression (1) is performed in two steps. First of all it is performed as the circular convolution of \mathbf{c} and $\mathbf{s}_{ex}[m]$ for obtaining $\mathbf{C}_f \mathbf{s}_{ex}[m]$. Subsequently, it is applied an iFFT of size $(MN \times MN)$ to the result of the first step for obtaining the vector $\mathbf{x}[m]$ of size $(MN \times 1)$. It is useful to comment that the computational complexity represented in (1) is dominantly determined by an iFFT of dimension $(MN \times MN)$. The $\mathbf{C}_f \mathbf{s}_{ex}[m]$ procedure can be calculated by:

$$\mathbf{C}_f \mathbf{s}_{ex}[m] = \mathbf{W}_{MN}[(\mathbf{W}_{MN}^{-1} \mathbf{c}) \odot (\mathbf{W}_{MN}^{-1} \mathbf{s}_{ex}[m])], \quad (2)$$

where \odot is an operator denoting the point-wise multiplication, and the circular convolution of the vectors \mathbf{c} and $\mathbf{s}_{ex}[m]$ are performed through point-wise multiplication of their respective iDFTs and later it is applied applying a DFT to the result. If one considers the expressions (1) and (2) the vector $\mathbf{x}[m]$ reduces to:

$$\mathbf{x}[m] = \mathbf{k} \odot (\mathbf{W}_{MN}^{-1} \mathbf{s}_{ex}[m]) \quad (3)$$

where $\mathbf{k} = \mathbf{W}_{MN}^{-1}\mathbf{c}$ is the vector of the prototype filter coefficients that to influencing on the GFDM performance. The computational complexity in (3) can be reduced significantly by taken into consideration that the vector $\mathbf{s}_{ex}[m]$ is the expanded version of the vector symbol $\mathbf{s}[m]$. However, the $\mathbf{W}_{MN}^{-1}\mathbf{s}_{ex}[m]$ product can be obtained by M repetitions of $\mathbf{W}_N^{-1}\mathbf{s}[m]$ in a column. Then the computational complexity in (3) can be calculated through an iFFT of dimension $(N \times N)$.

The data symbols \mathbf{s} of the GFDM packet to transmit in Figure 2 can be obtained by superposition of the M vectors $\mathbf{x}[m]$. We can describe this operation mathematically as:

$$\mathbf{x}_G = \sum_m^{M-1} \text{circshift}(\mathbf{x}[m], mN) \quad (4)$$

where $\text{circshift}(\cdot)$ means downward circular shift. The packet to transmit is completed by adding the CP samples to obtain the vector \mathbf{x}_G^{cp} . An interesting model in GFDM system is a matrix model with the aim to have likeness with the OFDM system. The model presented in [17–22] and the vector \mathbf{x}_G can be expressed in matrix form as:

$$\mathbf{x}_G = \mathbf{A}\mathbf{s} \quad (5)$$

where \mathbf{s} is the column vector that contains all the data symbols of the GFDM packet of M time slots and N subcarrier as is illustrated in Figure 2. \mathbf{A} is the matrix of the GFDM system that is composed by the coefficient of the prototype filter c_f that affect the performance of the system. The c_f coefficient will be calculated in other section.

2.2. Receiver Implementation

The vector \mathbf{x}_G is the output of the GFDM modulator (see Figure 3), \mathbf{x}_G contains the transmitted samples that correspond to the GFDM data block \mathbf{s} of size $(MN \times 1)$. Finally, we added on the transmitter side a cyclic prefix of L_{CP} samples to produce \mathbf{x}_G^{cp} . After that, the signal is affected by the Additive Gaussian White Noise (AWGN), $n \sim \mathcal{CN}(0, \sigma_n^2 \mathbf{I}_{MN})$, where σ_n^2 is the noise variance. The receiver signal after CP samples removal can be expressed as:

$$\mathbf{y}_G = \mathbf{H}\mathbf{A}\mathbf{s} + \mathbf{n} \quad (6)$$

where \mathbf{H} represents the circular matrix of the channel of size $(MN \times MN)$. The first column is shaped by the vector $\mathbf{h}_{ch} = [h_0 h_1 h_2 \dots h_{ch-1}]^T$ that corresponds to the impulse response of the discrete low-pass filter equivalent to the channel of size ch (completed with zeros). The circular matrix, \mathbf{H} , can be expressed as:

$$\mathbf{H} = \begin{bmatrix} h_0 & 0 & \dots & 0 \\ \vdots & h_0 & \ddots & 0 \\ h_{ch-1} & \vdots & \ddots & 0 \\ 0 & h_{ch-1} & \ddots & \vdots \\ 0 & 0 & \dots & h_0 \end{bmatrix} \quad (7)$$

From the matrix as represented by equation (6), we can use two standard GFDM receiver types, i.e. Zero Forcing (ZF) and Matched Filter (MF) receiver [4, 22, 23]. We has defined the \mathbf{B} matrix as the product of the \mathbf{H} and \mathbf{A} . Then equation (6) can be rewritten as:

$$\mathbf{y}_G = \mathbf{B}\mathbf{s} + \mathbf{n} \quad (8)$$

The equalization scheme employed in this work is presented in Figure 4. In the block scheme $\mathbf{Q}(\cdot)$ is a function that maps each component of the transmitted signal vector to the symbol nearest to the signal constellation of the modulation employed and $\mathbf{D}(\cdot)$ determines the minimum distance of the estimative first that is employed like a metric in the PIC detector. The switch in the figure defines the receiver employed in each state to obtain the final estimate. Here ZF and MF are linear detectors and PIC is the Parallel Interference Cancellation detector, respectively. Hence, the PIC is employed as a first estimation of the output signal of the MF block.

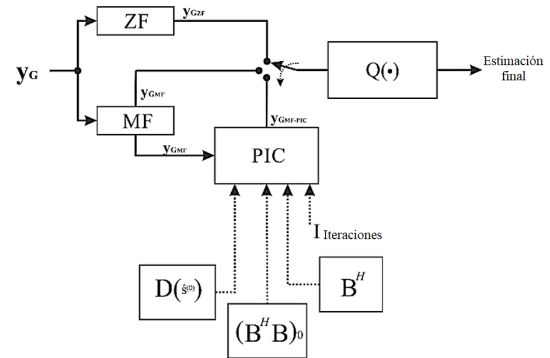


Figure 4. Block diagram of the receiver for GFDM.

The ZF receiver is characterized by the \mathbf{B}_{ZF} matrix that represents the \mathbf{B} inverse matrix. After obtaining the ZF equalization, the linear demodulation of the received signal can be expressed as:

$$\mathbf{y}_{GZF} = \mathbf{B}_{ZF}(\mathbf{B}\mathbf{s} + \mathbf{n}) = \mathbf{s} + \mathbf{n}_{ZF} \quad (9)$$

where $\mathbf{n}_{ZF} = \mathbf{B}_{ZF}\mathbf{n}$ is the noise after the ZF equalization that affects the received signal of size $(MN \times 1)$.

The second type receiver, i.e. the MF, is described by the $\mathbf{B}_{MF} = \mathbf{B}^H$ matrix. When it is applied the received vector in (8), the received signal can be expressed as:

$$\mathbf{y}_{G_{MF}} = \mathbf{B}_{MF}(\mathbf{B}\mathbf{s} + \mathbf{n}) = \mathbf{B}_{MF}\mathbf{B}\mathbf{s} + \mathbf{n}_{MF} \quad (10)$$

where $\mathbf{n}_{MF} = \mathbf{B}_{MF}\mathbf{n}$ is the noise after the MF equalization of size $(MN \times 1)$.

The PIC detector implementation presents the least computational complexity as compared with other cancellation detectors as SIC [17–20]. The first estimation of the data symbols to the PIC detector is obtained as the output signal of the MF detector. This receiver can be implemented by the equations:

$$\hat{\mathbf{s}}^{(j)} = Q(\mathbf{r}^{(j-1)}), j = 1, 2, \dots, \quad (11)$$

$$\mathbf{r}^{(j-1)} = \mathbf{B}^H \mathbf{y}_G - (\mathbf{B}^H \mathbf{B})_z \hat{\mathbf{s}}^{(j-1)}, j = 1, 2, \dots, \quad (12)$$

where $(\mathbf{B}^H \mathbf{B})_z$ corresponds to the matrix $\mathbf{B}^H \mathbf{B}$ with zeros in the main diagonal.

Symbols estimation using equations (11) and (12) are sequentially generated up to a maximum number, J , of iterations. In the present work it was considered that the process can be interrupted after j -th iterations ($1 \leq j \leq J$) depending on the quality of the generated estimates. The Maximum Likelihood (ML) metric employed here corresponds to the Minimum Distance (MD) metric. It can be computed as:

$$MD(\hat{\mathbf{s}}^{(j)}) = \|\mathbf{y}_G - \mathbf{B}\hat{\mathbf{s}}^{(j)}\|^2 \quad (13)$$

If one detects a reduction in the quality of a given estimate, that is, $MD(\hat{\mathbf{s}}^{(j)}) \geq MD(\hat{\mathbf{s}}^{(j-1)})$, the estimate $MD(\hat{\mathbf{s}}^{(j-1)})$ is adopted as the final one.

2.3. Calculating Filter Coefficients of the Subcarriers

The filtered of the subcarriers in the GFDM modulator block presented in Figure 3 is essential to the performance of the system. In this section presented like determine its coefficients. It is presented in [16, 24–26] the prototype filter corresponding to a class of real low-pass filters whose impulse response can be express as:

$$f_p[n] = \begin{cases} c_0 + 2 \sum_{l=1}^{F-1} c_l \cos\left(\frac{2\pi ln}{P}\right), & 0 \leq n \leq P \\ 0, & \text{otherwise} \end{cases} \quad (14)$$

where $P = FK$, and $c_l (0 \leq l < F)$ are real coefficients, the overlap factor F is a positive integer and K is the number of channels in the TMUX system.

The requirements for the coefficients $c_l (0 \leq l < F)$, after Mirabbasi and Martin [25] should meet the following conditions:

$$\begin{cases} c_0 = 1 \\ c_l^2 + c_{F-l}^2, & l = 1, 2, \dots, F/2 \end{cases} \quad (15)$$

If coefficients c_l are chosen such that expression in (15) hold, then the -3 dB frequency of the prototype filter would be approximately $\frac{\pi}{P}$, when F is even. The minimum stopband attenuation (MSA) and the approximate rate of fall-off (ARF) of the sidelobes depend of the overlap factor F and independent of the filter order [25].

It is required to find the F coefficients c_l , and to solve a system for determining F coefficients c_l . It was obtained in [24] the auxiliary equation:

$$c_0 + 2 \sum_{l=1}^{F-1} c_l = 0 \quad (16)$$

If equation (16) is satisfied, then the side lobes of the discrete Fourier transform in equation (14) have the approximate fall-off rate of $|\omega|^{-3}$, with ω defining the uniformly-spaced frequencies around the unit circle. It can be written as:

$$\omega_l = \frac{2\pi l}{P} \quad (l \text{ is an integer number}) \quad (17)$$

By using equations (15) and (16) it is possible to construct a system of equations with the same number of unknowns. Furthermore, equation (18) can be used to construct the remaining equations necessary to have a system of F equations.

$$\sum_{l=1}^{F-1} l^q c_l = 0, \quad q \geq 2 \quad (18)$$

with the above equations it is possible to obtain the values of the prototype filter coefficients for $F = 2$, $F = 3$ and $F = 15$. These are shown in the Table 1.

Table 1. Coefficients of the prototype Filter \mathbf{F}

Coefficients	$F = 2$	$F = 3$	$F = 15$
c_0	1	1	1
c_1	-0,7071	-0,9114	-0,9999
c_2		0,4114	0,9992
c_3			-0,988
c_4			0,9435
c_5			-0,8797
c_6			0,8328
c_7			-0,7628
c_8			0,6466
c_9			-0,5536
c_{10}			0,4755
c_{11}			-0,3313
c_{12}			0,1543
c_{13}			-0,0412
c_{14}			0,0048

3. Results and Discussions

The simulation results along with the derived theoretical obtained expressions are presented in this section. In order to study the effect of the filter coefficients quantity of the subcarrier on the BER in the system GFDM, we have considered the case of the ZF, MF and MF-PIC receivers.

3.1. BIT Error Rate Analysis

In this subsection we analyze the performance of the GFDM system in terms of BER versus E_b/N_0 assuming that ZF, MF and MF-PIC are employed. The ZF is able to remove self-generation interference at the cost of introducing noise enhancement [1]. The MF-PIC receiver was the most flexible and adaptable to different configurations of the data package GFDM [17, 18] as described in Figure 1. The system parameters used for the simulations are presented in Table 2, while Table 3 shows the channel impulse response used in the BER performance evaluation. The impulse response of the multipath channel is normalized to unitary energy and the length of the CP guard band is $G = ch$.

Table 2. System Parameters

Parameters	GFDM (I)	GFDM (II)
Modulation	4-QAM	4-QAM
Channel (ch)	6	8
Times-slots \times Subcarrier ($M \times N$)	4×64	16×32
Quantify of transmitted symbols	$76,8 \times 10^6$	$153,6 \times 10^6$
Quantify of filter coefficients (F)	2,3,15	-, -, 15

Table 3. Channel Model

Channel	Discrete impulse response (I)	Discrete impulse response (II)
Multipath Channel	0,7774	0,6961
	0,4905	0,501
	0,3095	0,3605
	0,1953	0,2595
	0,1232	0,1867
	0,0777	0,1343
	-	0,097
	-	0,0696

Figure 5 compares the BER performance of the classical ZF in the system GFDM with different quantity of filter coefficients of the subcarriers considering the system parameters from Table 2 and the multipath channel from Table 3. The results presented in Figure 5 suggest that the system GFDM achieved the best

performance when $F = 3$. In this case the Bit Error Rate was in the order of 2×10^{-2} , when compared to the results presented for $F = 2$ while $F = 15$ had more than 3 dB of advantage.

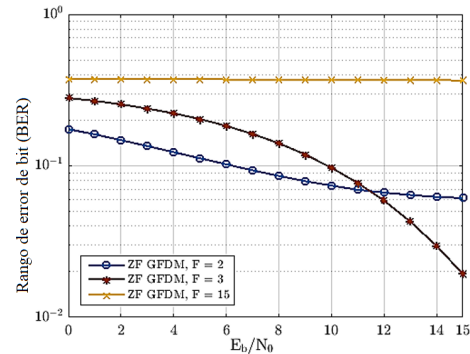


Figure 5. BER simulation result for ZF receiver in GFDM (I), channel I.

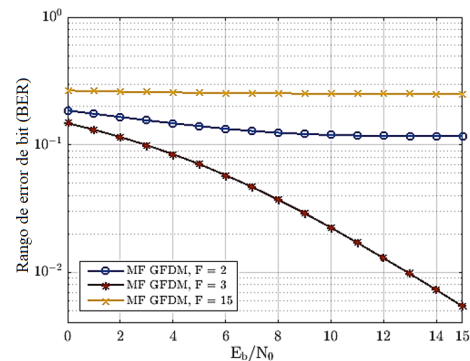


Figure 6. BER simulation result for MF receiver in GFDM (I), channel I.

Figures 6 and 7 illustrate the BER performance for the MF and MF-PIC receivers considering the three F cases. The figures showed that performance of the system GFDM depends strongly on the quantity of coefficients of the prototype filter of the subcarriers. The case $F = M - 1$ rendered the best choice of the quantity of filter coefficients in the system GFDM. Here, M represents the time slots of the system as depicted in Figure 2.

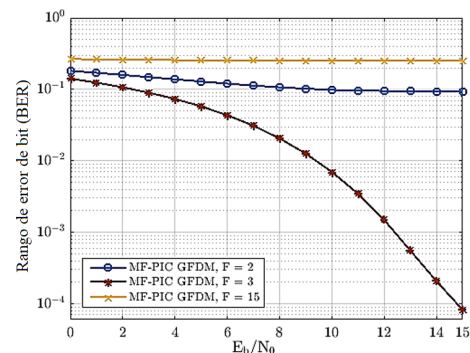


Figure 7. BER simulation result for MF-PIC receiver in GFDM (I), channel I.

The results shown in Figure 8 suggest that employing $F = 3$ for the different receivers the MF-PIC detector had the best performance of the GFDM system. We found that the MF receiver is 4 dB more efficient than ZF with less computational complexity. The MF-PIC is more complex than ZF and MF due to the number of iterations [18]. Furthermore, in Figure 8 we present (as a comparison) two curves of the performance, a 4-QAM theoretical and other ZF CP-OFDM with 64 FFT. It is found that BER performance of the MF-PIC scheme is approximately the same with ZF CP-OFDM FFT 64, where the difference in the performance is 0,5 dB in favor of the CP-OFDM system. The cause behind this small difference is that the GFDM system is affected by the transmission matrix that depends on the coefficients quantity. However, both systems have the same computational complexity in the signal generation as they need FFT 64 but GFDM is more efficient than OFDM in terms of spectrum because the need of just only one CP to transmit a data packet of 256 symbols. On the other hand, the great difference in the BER performance of the 4-QAM is produced because it is considered as a system with AWGN.

In the simulations both systems have the same computational complexity in the signal generation as they need FFT 64 but GFDM is more efficient than OFDM in terms of spectrum because the need of just only one CP to transmit a data packet of 256 symbols.

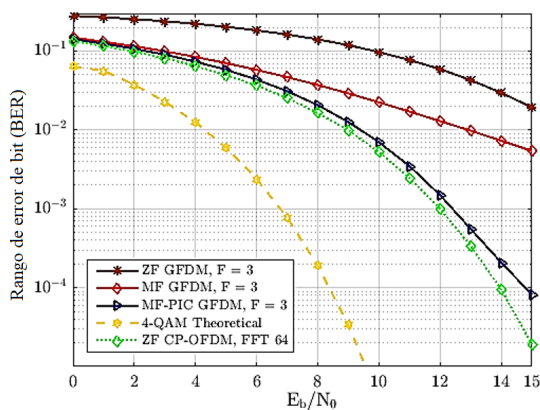


Figure 8. Comparison of the simulation result for ZF, MF and MF-PIC receiver in GFDM (I) with $F=3$, 4-QAM Theoretical and ZF CP-OFDM FFT 64, channel I.

Other simulations are presented in Figure 9 considering that the GFDM system has dimension matrices (512×512) and the properties described in Table 2 for GFDM (II). The impulse responses of the channel have 8 taps like exhibited in Table 3. Figure 9 is shown that performance of the MF-PIC scheme detector is approximately the same with ZF CP-OFDM FFT 32, where the difference in the performance is 0,5 dB in favor of the CP-OFDM system. Here, it is possible to verify again that there is an intrinsic relationship with

the total coefficients of the subcarrier filter, because the best performance that can reach the GFDM system is equal to the OFDM system. The degradation of the performance in Figure 9 in comparison with Figure 8 is given by channel effect by increase the number of taps.

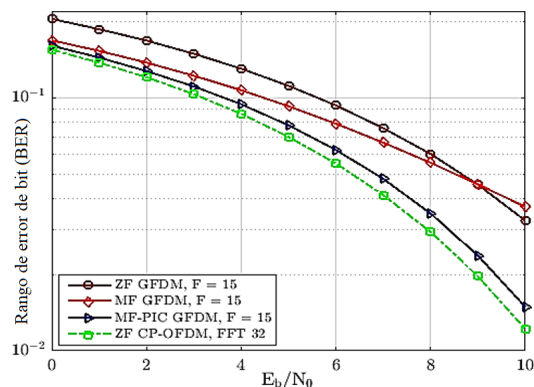


Figure 9. Comparison of the simulation result for ZF, MF and MF-PIC receiver in GFDM (II) with $F=15$ and ZF CP-OFDM FFT 32, channel II.

4. Conclusions

The expected implementation scenarios for the 5G wireless networks have challenges as the available physical layer technologies show a limited performance due to their shortcoming. The GFDM system seems a useful candidate by its rendering with the OFDM system. The key property of the GFDM system is the flexibility such that different applications can have a simple solution. This way, it is important to guarantee the coexistence with other technologies, as the current 4G.

We produced modulation and demodulation schemes for GFDM system. The presented schemes have a matrix structure that reduces the computational complexity without incurring in any performance loss penalty. By employing the matrix structure of the transmitter and receiver GFDM systems, we analyzed and compared the BER performance for the different calculated coefficients. It was shown that the BER performance of the GFDM system depends on the coefficients quantity of the filter and prototype filter. In the GFDM system, to increase the total number of the coefficient's filter not improve the performance in the GFDM system. The coefficient total depends on the number of subcarriers because it might filter symbols of others packets and generates interference. The performance of the system is conditional on accurate the coefficient total.

References

- [1] N. Michailow, M. Matthé, I. S. Gaspar, A. N. Caldevilla, L. L. Mendes, A. Festag, and G. Fettweis, "Generalized frequency division multiplexing for 5th generation cellular networks," *IEEE Transactions on Communications*, vol. 62, no. 9, pp. 3045–3061, Sep. 2014. [Online]. Available: <https://doi.org/10.1109/TCOMM.2014.2345566>
- [2] E. Öztürk, E. Basar, and H. A. Çirpan, "Generalized frequency division multiplexing with flexible index modulation," *IEEE Access*, vol. 5, pp. 24 727–24 746, 2017. [Online]. Available: <https://doi.org/10.1109/ACCESS.2017.2768401>
- [3] G. Wunder, P. Jung, M. Kasparick, T. Wild, F. Schaich, Y. Chen, S. T. Brink, I. Gaspar, N. Michailow, A. Festag, L. Mendes, N. Cassiau, D. Ktenas, M. Dryjanski, S. Pietrzyk, B. Eged, P. Vago, and F. Wiedmann, "5gnow: non-orthogonal, asynchronous waveforms for future mobile applications," *IEEE Communications Magazine*, vol. 52, no. 2, pp. 97–105, February 2014. [Online]. Available: <https://doi.org/10.1109/MCOM.2014.6736749>
- [4] L. Sendrei and S. Marchevský, "On the performance of gfdm systems undergoing nonlinear amplification," *Acta Electrotechnica et Informatica*, vol. 15, no. 1, pp. 9–14, 2015. [Online]. Available: <http://doi.org/10.15546/aei-2015-0002>
- [5] S. K. Bandari, V. M. Vakamulla, and A. Drosopoulos, "Gfdm/oqam performance analysis under nakagami fading channels," *Physical Communication*, vol. 26, pp. 162–169, 2018. [Online]. Available: <https://doi.org/10.1016/j.phycom.2017.12.008>
- [6] F. Schaich and T. Wild, "Waveform contenders for 5g – ofdm vs. fbmc vs. ufmc," in *2014 6th International Symposium on Communications, Control and Signal Processing (ISCCSP)*, May 2014, pp. 457–460. [Online]. Available: <https://doi.org/10.1109/ISCCSP.2014.6877912>
- [7] A. N. Ibrahim and M. F. L. Abdullah, "The potential of fbmc over ofdm for the future 5g mobile communication technology," *AIP Conference Proceedings*, vol. 1883, no. 1, p. 020001, 2017. [Online]. Available: <https://doi.org/10.1063/1.5002019>
- [8] E. Öztürk, E. Basar, and H. A. Çirpan, "Spatial modulation gfdm: A low complexity mimo-gfdm system for 5g wireless networks," in *2016 IEEE International Black Sea Conference on Communications and Networking (BlackSeaCom)*, 2016, pp. 1–5. [Online]. Available: <https://doi.org/10.1109/BlackSeaCom.2016.7901544>
- [9] A. Farhang, N. Marchetti, and L. E. Doyle, "Low-complexity modem design for gfdm," *IEEE Transactions on Signal Processing*, vol. 64, no. 6, pp. 1507–1518, March 2016. [Online]. Available: <https://doi.org/10.1109/TSP.2015.2502546>
- [10] A. M. Tonello and M. Girotto, "Cyclic block fnt modulation for broadband power line communications," in *2013 IEEE 17th International Symposium on Power Line Communications and Its Applications*, March 2013, pp. 247–251. [Online]. Available: <https://doi.org/10.1109/ISPLC.2013.6525858>
- [11] G. Fettweis, M. Krondorf, and S. Bittner, "Gfdm - generalized frequency division multiplexing," in *VTC Spring 2009 - IEEE 69th Vehicular Technology Conference*, April 2009, pp. 1–4. [Online]. Available: <https://doi.org/10.1109/VETECS.2009.5073571>
- [12] H. Lin and P. Siohan, "An advanced multi-carrier modulation for future radio systems," in *2014 IEEE International Conference on Acoustics, Speech and Signal Processing (ICASSP)*, May 2014, pp. 8097–8101. [Online]. Available: <https://doi.org/10.1109/ICASSP.2014.6855178>
- [13] M. Renfors, J. Yli-Kaakinen, and F. J. Harris, "Analysis and design of efficient and flexible fast-convolution based multirate filter banks," *IEEE Transactions on Signal Processing*, vol. 62, no. 15, pp. 3768–3783, Aug 2014. [Online]. Available: <https://doi.org/10.1109/TSP.2014.2330331>
- [14] A. Farhang, N. Marchetti, L. E. Doyle, and B. Farhang-Boroujeny, "Filter bank multicarrier for massive mimo," in *2014 IEEE 80th Vehicular Technology Conference (VTC2014-Fall)*, Sep. 2014, pp. 1–7. [Online]. Available: <https://doi.org/10.1109/VTCSFall.2014.6965986>
- [15] R. Datta and G. Fettweis, "Improved aclr by cancellation carrier insertion in gfdm based cognitive radios," in *2014 IEEE 79th Vehicular Technology Conference (VTC Spring)*, May 2014, pp. 1–5. [Online]. Available: <https://doi.org/10.1109/VTCSpring.2014.7022943>
- [16] B. Farhang-Boroujeny and H. Moradi, "Derivation of gfdm based on ofdm principles," in *2015 IEEE International Conference on Communications (ICC)*, June 2015, pp. 2680–2685. [Online]. Available: <https://doi.org/10.1109/ICC.2015.7248730>
- [17] R. Verdecia Peña, R. Pereira David, and R. Sampaio-Neto, "Detecção de sinais e estimação de canal em sistemas gfdm," in *XXXVII Simpósio Brasileiro de Telecomunicações e Processamento de Sinal SBrT2019, At: Petrópolis, RJ*, 2019. [Online]. Available: <https://bit.ly/34VPa17>

- [18] R. Verdecia Peña, “Análise espectral, detecção de sinais e estimação de canal em sistemas GFDM,” Master’s thesis, 2019. [Online]. Available: <https://bit.ly/34LM96N>
- [19] J. P. Mayoral Arteaga, “Detecção de sinais em sistemas com transmissão gfdm,” Master’s thesis, 2017. [Online]. Available: <https://bit.ly/2DEbbc2>
- [20] J. P. Mayoral Arteaga, R. Pereira David, and R. Sampaio Neto, “Simultaneous detection and parallel interference cancellation in GFDM for 5G,” in *XXXV Simposio brasileiro de telecomunicações e processamento de sinais - SBRT2017, 3-6 de setembro de 2017, São Pedro, SP*, 2017, pp. 220–224. [Online]. Available: <https://bit.ly/387wqRF>
- [21] R. Verdecia Peña, “Análisis del desempeño de los esquemas de modulación BPSK y QPSK para diferentes condiciones de canales en sistema GFDM,” *MASKAY*, vol. 8, no. 1, pp. 7–112, 2018. [Online]. Available: <http://dx.doi.org/10.24133/maskay.v8i1.506>
- [22] —, “Desempeño de los métodos de detección de señales con modulación QPSK en sistema GFDM para 5G.” *Revista Cubana de Ciencias Informáticas*, vol. 12, pp. 104–120, 09 2018. [Online]. Available: <https://bit.ly/33GWbo9>
- [23] N. Michailow, R. Datta, S. Krone, M. Lentmaier, and G. Fettweis, “Generalized frequency division multiplexing: A flexible multi-carrier modulation scheme for 5th generation cellular networks,” 2012. [Online]. Available: <https://bit.ly/2rQep9B>
- [24] N. Michailow, S. Krone, M. Lentmaier, and G. Fettweis, “Bit error rate performance of generalized frequency division multiplexing,” in *2012 IEEE Vehicular Technology Conference (VTC Fall)*, Sep. 2012, pp. 1–5. [Online]. Available: <https://doi.org/10.1109/VTCFall.2012.6399305>
- [25] S. Mirabbasi and K. Martin, “Overlapped complex-modulated transmultiplexer filters with simplified design and superior stopbands,” *IEEE Transactions on Circuits and Systems II: Analog and Digital Signal Processing*, vol. 50, no. 8, pp. 456–469, Aug 2003. [Online]. Available: <https://doi.org/10.1109/TCSII.2003.813592>
- [26] K. W. Martin, “Small side-lobe filter design for multitone data-communication applications,” *IEEE Transactions on Circuits and Systems II: Analog and Digital Signal Processing*, vol. 45, no. 8, pp. 1155–1161, Aug 1998.